Vertical density gradient in the eastern North Atlantic during the last 30,000 years.

Rogerson, M[1]., Bigg, G.R.[2], Rohling, E.J[3]. and Ramirez, J[1].

[1] Geography Department, University of Hull, Cottingham Road, Hull, HU6 7RX, UK, m.rogerson@hull.ac.uk

[2] Department of Geography, University of Sheffield, Winter Street, S10 2TN, grant.bigg@sheffield.ac.uk

[3] School of Ocean and Earth Science, University of Southampton, National Oceanography Centre Southampton, SO14 3ZH, e.rohling@noc.soton.ac.uk

Abstract.

Past changes in the density and momentum structure of oceanic circulation are an important aspect of changes in the Atlantic Meridional Overturning Circulation and consequently climate. However, very little is known about past changes in the vertical density structure of the ocean, even very extensively studied systems such as the North Atlantic. Here we exploit the physical controls on the settling depth of the dense Mediterranean water plume derived from the Strait of Gibraltar to obtain the first robust, observations-based, probabilistic reconstruction of the vertical density gradient in the eastern North Atlantic during the last 30,000 years. We find that this gradient was weakened by more than 50%, relative to the present, during the last Glacial Maximum, and that changes in general are associated with reductions in AMOC intensity. However, we find only a small change during Heinrich Event 1 relative to the Last Glacial Maximum, despite strong evidence that overturning was substantially altered. This implies that millennial-scale changes may not be reflected in vertical density structure of the ocean, which may be limited to responses on an ocean-overturning timescale or longer. Regardless, our novel reconstruction of Atlantic density structure can be used as the basis for a dynamical measure for validation of model-based AMOC reconstructions. In addition, our general approach is transferrable to other marginal sea outflow plumes, to provide estimates of oceanic vertical density gradients in other locations.

Atlantic Ocean: Meridional Overturning: Overflow Physics: Mediterranean Outflow: Iberian Margin: Paleoceanography

Introduction

Progress in the reconstruction of past Atlantic Meridional Overturning Circulation (AMOC) changes (McManus et al. 2004; Robinson et al. 2005; Hall et al. 2006; Stanford et al. 2006; Lynch-Stieglitz et al. 2007) has revealed that AMOC reductions coincided with colder episodes within the Last Glacial, especially Heinrich Events (McManus et al. 2004; Robinson et al. 2005). Also, a prominent chemocline has been identified at around 2000m depth in the North Atlantic during the Last Glacial Maximum (LGM) and Heinrich Event 1 (H1) (Robinson et al. 2005; Grootes et al. 2008), which suggests an altered deep-water circulation state. However, so far hardly anything is known about the past subsurface density structure in the North Atlantic. As this structure is fundamental for understanding deep-water circulation (Lynch-Stieglitz et al. 2007), it is critically important that new means are established for assessing changes in oceanic vertical density structures. We present new insight into this structure in the eastern North Atlantic from a novel approach that centres on the physical controls on depth-changes of the Mediterranean Outflow plume through time.

The settling depth of the plume of dense water that results from subsurface outflow from the Mediterranean through the Strait of Gibraltar (Atlantic Mediterranean Water; AMW) is controlled by: *(1)* the density anomaly of pure Mediterranean Outflow Water (MOW) at its exit from the Strait of Gibraltar (SoG); *(2)* the degree of mixing this water experiences as it descends down the slope of the Gulf of Cadiz; and *(3)* the density structure of the Atlantic Ocean to the west of the Gulf of Cadiz (O'Neill-Baringer and Price 1997). The density anomaly of pure MOW (relative to ambient North Atlantic waters) has varied through time, mainly due to hydraulic controls imposed by changes in eustatic sea level on the geometry of the SoG (Rogerson et al. 2005), with second-order influences from regional climate changes (Voelker et al. 2006; Rogerson et al. 2010).

Globally cold periods such as the LGM and H1 coincide with generally low sea levels (130-60 m below present) (Siddall et al. 2003), high buoyancy loss from the northwest Mediterranean (Hayes et al. 2005; Kuhlemann et al. 2008), and consequently very dense MOW (Rogerson et al. 2005). During those times, the AMW plume settled at a much greater depth than today, as evidenced by a withdrawal of flow from the upper slope of the Gulf of Cadiz and enhanced flow on the lower slope (Rogerson et al. 2006; Voelker et al. 2006). A prominent sedimentary unconformity, significant changes in benthic foraminiferal isotopes, and distinct palaeoecological changes (Schönfeld and Zahn 2000) on the Portuguese margin between 1700 and 2000 m depth, indicate that AMW influences reached to at least those depths during the LGM. Stable isotope data from the Portuguese margin suggest that AMW influences even reached down to ~2600m during Heinrich Stadials (Skinner and Elderfield 2007). In contrast, the core of the AMW plume today resides at ~800m, with the very deepest AMW influences around 1700m (O'Neill-Baringer and Price 1999).

Overall, to satisfy the whole range of evidence from sedimentary records, it appears that the core of the AMW resided at least 900m deeper during glacial times than today (Rogerson et al. 2005) (Fig. 1a). Although the intuitive expectation would be that denser MOW produces a denser AMW plume that settles at greater depths, this expectation is incorrect. Instead, it has been well established that denser MOW leads to a higher plume velocity, which in turn drives enhanced ambient water entrainment during settling. This is a negative feedback process that is ubiquitous in overflow plumes (Price and O'Neill-Baringer 1994). Thus, an enhanced glacial density contrast at the SoG would result in either a negligible change in the AMW plume settling depth, or even a reduction (Price and O'Neill-Baringer 1994). Here, we quantitatively evaluate the controls on past AMW settling depth to explain the apparent contradiction between theoretical and observational constraints on the system.

Methods

We quantify the Mediterranean Outflow and entrainment system concept using a widely accepted theory of marginal sea overflow mixing (Price and O'Neill-Baringer 1994), coupled with a somewhat modified version of a model for the Gibraltar

Exchange (Bryden and Kinder 1991). We will refer to these two models as "PO94" and "BK91" respectively. Because glacial conditions cannot be specified without considerable uncertainty, we instead present our analysis of controls on the AMW settling depth in a Monte Carlo-style approach across a broad parameter space of possible conditions. The Mediterranean excess of evaporation over total freshwater input (X_{Med}), temperature loss during conversion of Atlantic Inflow to Mediterranean Intermediate and Deep Waters and sea level are all allowed to vary independently, simultaneously and randomly, with the only constraint being that deep water in the Western Mediterranean must be of higher density (i.e. lower temperature) than intermediate water. Each experiment comprises 5,000 iterations of the model.

The PO94 model assumes that entrainment of ambient water occurs as a single event around 100km downstream of the Camarinal sill, mixing a single type of Mediterranean water and a single type of ambient water to produce a single type of product water (Price and O'Neill-Baringer 1994). It does not account for differential mixing due to Ekman veering (O'Neill-Baringer and Price 1997). Consequently, this model provides only a single product water density, which in essence identifies the mean isopycnal on which the final AMW will settle. The critical parameter for PO94 is the "proportional mixing coefficient"

$$\Phi = 1 - (B_{geo}^{1/3} / U_{geo})$$

where B_{geo} is the geostrophic buoyancy flux of the AMW plume and U_{geo} is the geostrophic velocity. These parameters are given by

$$U_{geo} = (g' \pi / f)$$
$$B_{geo} = (H_{src} U_{src} g') / (1 + 2K_{geo} x / W_{src}),$$

where π is the gradient of the continental slope, f is the Coriolis parameter (0.000084), x is the distance downstream from Gibraltar (100km), and g' is the reduced gravity of pure MO water ($g' = (g\ \rho_{MO} - \rho_{ATL}) / \rho_{MO}$) where ρ_{MO} and ρ_{ATL} are the densities of Mediterranean Outflow and Atlantic water). H_{src}, W_{src}, U_{src} are the height, width and velocity of the flow at the Camarinal Sill, g is the acceleration due to gravity, and K_{geo}

is the geostrophic Ekman number that is generally ≤0.2 (PO94). Today, $\Phi = 0.58$, meaning that AMW comprises 42% Mediterranean Water (PO94), which is of similar order as estimates from direct measurement (~33%) (O'Neill-Baringer and Price 1999). The difference between the observed and modelled values for entrainment results in the AMW plume in the model having density enhanced by ~1.27×10^{-4} kg m^{-3}, which is ~7.5% of the initial density anomaly of pure MOW and therefore negligible. The necessary input parameters for assessment of past changes in Φ therefore relate to the geometry of the flow in the SoG (H_{src}, U_{src} and W_{src}) and the reduced density of pure Mediterranean Outflow water (g').

The required geometric parameters represent conditions at the shallowest point in the Strait of Gibraltar, the Camarinal sill, which is the location of hydraulic control on the outflow (Armi and Farmer 1988). W_{src} is altered by changes in water depth above the sill and thus is a function of global sea level. W_{src} is estimated on the basis of sea-level influences on the triangular cross section of the sill section with a width of 20km and a depth of 284m (Bryden and Kinder 1991). U_{src} depends on the sea floor gradient in the direction of flow over the shallowest part of the sill, the g' of MO water, and (on short time scales) on a range of tidal and subinertial forces. Given that the average variability in U_{src} on timescales above decadal is not sensitive to the latter's short-term influences (Gomis et al. 2006), changes in U_{src} may be viewed as forced only by changes in g'. This perspective is further enhanced by the observation that flow over the westernmost sill within the Gibraltar Strait system (the Spartel Sill) is almost constant throughout the tidal cycle (Bryden et al. 1988; Garcia-Lafuente et al. 2009). For any g', H_{src} can therefore be estimated from the relationship of flux (Q_{MO}) to velocity and cross sectional area. Consequently, the only boundary conditions we need to supply the PO94 model with are global sea level change, flux (Q_{MO}) and reduced density of pure Mediterranean water (g'). When these statements are combined, settling depth of the AMW plume is a simple estimate from:-

$$D_{settling} = (D_s - H') + \frac{(\Delta\rho_{MO} * \Phi)}{(\partial\rho / \partial z)}$$

Where $D_{settling}$ is the PO94 estimate of mean settling depth for the AMW plume in the Atlantic. This rearranges to

$$\partial\rho / \partial z = \frac{(\Delta\rho_{MO} * \Phi)}{D_{settling} - (D_s - H')}$$

providing a simple representation of eastern Atlantic vertical density gradient. Density is a property that varies quite smoothly in the ocean interior, especially westward of Gibraltar where the oceanography is essentially zonal due to the structure imposed by the Azores Front (Gould 1985; New et al. 2001; Alves et al. 2002). Consequently, we anticipate that the Gulf of Cadiz vertical density gradient will be representative at least of a region extending west to the Mid Atlantic ridge and north to the Bay of Biscay.

Following previous studies (Rogerson et al. 2005; Rogerson et al. 2006), we estimate the flux of outflowing Mediterranean Water at the Camarinal Sill (Q_{MO}), the vertical density difference at the sill ($\Delta\rho_{MW}$) and the initial reduced density of water mixing in the Gulf of Cadiz (*g*') using the model of Gibraltar exchange of Bryden and Kinder (1991; BK91). It expresses hydraulic control on flow through the sill and narrows sections of Gibraltar with mass and salt conservation (Bryden and Kinder 1991). We modify this model here in one important aspect, in that we include sensitivity of *g*' to changes in regional sea surface temperature gradients (BK91 model considered only salinity effects), as these are known to be variable on glacial-interglacial timescales (Kuhlemann et al. 2008). The BK91 requires an iterative solution for the relationship between ΔS_{gib} and Q_{total}, and we approach this by exploiting a convergent solution within the paired equations following the simplification provided by Mikolajewicz (Mikolajewicz 2010).

$$\Delta S_{gib} = S_{atl} (X_{med} / (0.5Q_{total} - X_{med}))$$

$$Q_{total} = ((C ((W_{src} D_s) / 2)) * \sqrt{}((\beta \Delta S_{gib} + \alpha \Delta T_{gib}) g D_s / \rho_{MO})$$

where C is a geometric coefficient representing the shape of the Strait of Gibraltar, β and α are the salinity contraction and thermal expansion coefficients respectively and ΔT_{gib} is the temperature difference between inflowing and outflowing water. Salinity of the inflowing Atlantic water is calculated directly from the proportional loss of global ocean volume due to eustatic sea level change ($S_{atl} = S_{atl\text{-}pres}\, H / [H - h']$). The temperature of the deep and intermediate water layers of Mediterranean water that pass over the sill (Mediterranean Dense Water {MDW} and Mediterranean Intermediate Water {MIW} respectively), respectively (Millot 2009)) are provided by arbitrary offsets (between 0 and 6^{o}C) from winter sea surface temperature in the Gulf of Cadiz. These offsets are randomly generated via a Monte Carlo approach and this variability is propagated through the rest of the model (see Table 1). Potential density of the Atlantic, MIW, and MDW watermasses are calculated from the model output salinity and temperature data and the Levitus and Isayev polynomial approximation of the equation of state for seawater (Levitus and Isayev 1992).

To simulate the impact of entraining sediment into the Mediterranean Outflow plume, which may be relevant to past changes in plume density, we exploit the relationship between bottom velocity and sediment entrainment, using a simple parameterisation (Karim and Kennedy 1990) known to be relatively insensitive to errors in estimation of velocity and grainsize (Pinto et al. 2006). The equation for q_s, the flux of sediment entrained, is

$$q_s = 10^{-2.821+33.69 \log(x1)+0.840 \log(x2)} \sqrt{((s_d - 1)\, g\, d_{50}^{3})}$$

where $x1 = U_{geo} / \sqrt{((s_d - 1)\, g\, d_{50})}$ and $x2 = (U^* - U^*_{crit}) / \sqrt{((s_d - 1)\, g\, d_{50})}$. Here, s_d is the density of the sediment (2.65 kg m^{-3}), , U^* is the bottom shear velocity ($U^* = \sqrt{(0.8 U_{geo}^{2})}$ and U^*_{crit} is the critical shear velocity for $d_{50} = 2.4$, which is taken from the Shields diagram (2.4) (Julien 1998). d_{50} is the median grainsize of the sediment available on the slope. We use 2.4μm for this parameter, which is taken from core top data (Rogerson et al. 2011) as there is insufficient data available for the sediment grainsize distribution on the slope during the LGM. As the MOW plume would have been smaller in the past (Rogerson et al. 2005), it is likely that, on the scale of the whole slope, the sediment available for erosion was slightly finer. As this would make the sediment more cohesive, raising U*crit, our assessment of the impact of sediment entrainment should be seen as representing the maximum likely value.

Results and Discussion

The results of our analysis (Fig. 1) reveal a significant positive relationship between AMW settling depth and density increase (buoyancy decrease) in the Mediterranean due to evaporation (Fig. 1b; $r^2 = 0.85$) but only a weak positive relationship with cooling (Fig. 1c, d) or sea level change (Fig. 1e). However, even within the generous bounds of parameter space investigated, changes in these parameters cannot make AMW settle more than ~200m below its present depth, despite the potential for up to 130m of displacement directly from sea level change alone.

Sediment entrainment may provide a mechanism for secondary enhancement of AMW density and consequently might promote greater settling depth, given that the flow's estimated shear velocities (Fig. 1f) mostly exceed the critical value (2.4 m s^{-1}) needed to allow strong sediment entrainment of fine silt grade sediment (McCave and Hall 2006). Indeed, we found that for shear velocities higher than ~6.8 m s^{-1} sediment entrainment resulted in concentrations >5% by volume (grey area, Fig. 1f). This level of suspension is generally considered as being "hyperconcentration" and such flows are known to exhibit reduced entrainment of sediment, possibly resulting in net deposition, in addition to having different mixing and flow hydraulics to "normal" flows of suspended sediment (Julien 1998). The physics represented in our model will thus overestimate continued entrainment beyond the 5% level, and as it is unlikely that such a flow would be capable of forming a geostrophic current (instead being more likely to behave like a conventional sedimentary turbidity current) we therefore enforce a maximum entrainment level of 5% for the fastest flows. Unless some form of hyperconcentrated flow is permitted, we again find that the large glacial settling depth increase (Fig. 1a) cannot be explained via sediment entrainment (Fig. 2a-c). In our simulations, the maximum impacts of sea-level, temperature and salinity changes within the Mediterranean, and suspended sediment influences, are an increase in settling depth of the AMW core of ~150m, which is insufficient to take even the lowermost AMW down to the depths observed for the LGM. A major additional control on settling depth is clearly dominating the system.

This leads us to the only remaining potential mechanism for explaining the deep glacial settling of the AMW core at depths of ~1700m or more, namely reduction of the vertical density gradient in the eastern North Atlantic. We investigate the influence of this parameter by varying it in our model between 0.1 and 2 times its modern value of 1.1 x 10^{-4} kg m^{-4} (Fig 2 d, e, f). This reveals that the observations of AMW influences at 2000m (with a core depth ~1700m) during the LGM (Schönfeld and Zahn 2000), and potentially even deeper during Heinrich Stadials (Skinner and Elderfield 2007), require a glacial vertical density gradient in the eastern North Atlantic that was reduced to less than half its present-day value (Fig. 2f).

To gauge whether such a change would be physically plausible, we have extracted glacial-interglacial changes in vertical density gradients in the region between 27-37^{o}N and 10-20^{o}W from existing simulations of the ocean part of the 'Frugal' climate model (Levine and Bigg 2008), one of the few climate models to actually represent the SoG as a proper strait. Area-mean σ_θ profiles across all model levels between 0 and 3000m depth systematically show somewhat lower absolute values than observed from hydrographic data, but the vertical structure agrees well in a relative sense (Fig. 3). The vertical density gradients for the LGM, and for a Heinrich Event (where 0.4Sv of freshwater equivalent in the form of icebergs was released from Hudson Strait; (Levine and Bigg 2008), are less than half the present-day gradient; over the 300-1000m depth range, where most of the conversion of MOW to AMW occurs (Price et al. 1993), the vertical gradient is 4.2 x 10^{-4} and 4.1 x 10^{-4} kg m^{-4} in the LGM and Heinrich simulations respectively, relative to 11 x 10^{-4} kg m^{-4} in the present-day simulation (Levine and Bigg 2008). These results demonstrate that our inference of a roughly 50% reduced vertical density gradient in the eastern North Atlantic is physically plausible. Moreover, this analysis confirms that the mechanism causing vertical density gradient reduction is linked to weakened AMOC transport. Given that AMOC and Atlantic vertical density gradients are both reflections of the buoyancy budget of the Atlantic, this relationship is not in itself surprising. High AMOC transport must physically coincide with strong buoyancy loss in the Nordic Seas region, and thus with very dense Atlantic interior waters and consequent very strong vertical density gradients. However, our new approach allows this relationship to be investigated directly from observations, providing powerful dynamical constraints to modelling studies of AMOC change.

The relative insensitivity of the AMW settling depth to parameters other than the Atlantic vertical density gradient allows us to assess the minimum change in density gradient that is compatible with the observed glacial-interglacial AMW settling-depth changes. Figure 4 shows a probabilistic assessment of the density gradient values necessary to achieve AMW flow at depths reported at selected periods over the last 30ka (Table 2). This reveals that the most likely density gradient during the LGM was ~3.1 x 10^{-4} kg m^{-4} with a $\pm 2\sigma$ range between 2.08 x 10^{-4} and 4.27 x 10^{-4} kg m^{-4}. The relative change from today equates to a 52-77% reduction, which encompasses the fractional reduction from the GCM simulations. Also shown in Figure 4 is the same assessment where sediment entrainment is considered (as above, hyperconcentrated flows are excluded) which indicates only minor modification of the Atlantic density gradients required, although the upper limit is higher (5.47 x 10^{-4} kg m^{-4}) implying a somewhat smaller reduction relative to the present than in the case without sediment entrainment. Also shown are scenarios for Heinrich Event 1, the Younger Dryas, Bölling-Alleröd and Holocene (see parameterisation in Table 2). There is a clear relationship with northern hemisphere climate, with colder periods exhibiting lower vertical density gradients. However, the Heinrich Event 1 scenario differs only marginally from the LGM scenarios, which stands in contrast to the considerable inferred change in AMOC (McManus et al. 2004; Robinson et al. 2005; Hall et al. 2006; Stanford et al. 2006; Lynch-Stieglitz et al. 2007). This implies that, unlike AMOC, the density structure cannot respond to millennial-scale forcing and that its response is limited to ocean-overturning timescales. This, in turn, implies that AMOC is not strictly tied to the Atlantic stratification on short (<1 ka) timescales, despite the common forcing outlined above.

Nevertheless, our reconstructions largely compare well with concepts of past AMOC change derived entirely from independent sources of palaeoceanographic data and general circulation models. Moreover, they provide a pivotal deep-water validation to concepts of the dynamically determined structure in the glacial eastern North Atlantic (Levine and Bigg 2008), and so of the glacial AMOC. Previously, model validation largely relied on the distribution of water-mass properties such as surface or benthic temperatures. Our reconstruction of the vertical density gradient – based on robust measurements and quantified using physical relationships – for the first time provides a critical reconstruction of dynamical structure within the ocean interior, for testing models of large-scale ocean circulation.

Conclusions

1) The settling depth of the Mediterranean Outflow plume is largely insensitive to changes in watermass properties in the Mediterranean Sea, even on glacial-interglacial timescales. Increased settling depth also cannot be related to sediment entrainment effects, unless the flow becomes super-concentrated, which would disagree with the strong geostrophic nature of the flow.

2) AMW settling depth therefore depends predominantly on the vertical density gradient in the eastern North Atlantic.

3) The eastern North Atlantic vertical density gradient is found to be reduced by more than 50% during the Last Glacial Maximum, compared to the present, which agrees well with previous reconstructions of AMOC intensity changes.

4) Little difference is found between the LGM and Heinrich Event 1. This implies there is a limitation to the speed of response of this parameter, which does not seem to alter on timescales lower than millennial-scale ocean overturning rate.

5) We have elaborated our plume-control approach in a case specific to the Mediterranean outflow, but it is in a general sense transferrable to other marginal seas. Hence, the general approach offers exciting opportunities for estimating oceanic vertical density gradients in many other sites where strait exchange can be modelled and outflow plume height changes through time can be reconstructed from shallow seismics and borehole studies.

Acknowledgements

We warmly acknowledge the assistance of three anonymous reviewers, whose comments improved the quality of this manuscript. EJR acknowledges support from a Royal Society-Wolfson Research Merit Award. This study contributes to Natural Environment Research Council projects NE/H004424/1, NE/I009906/1, NE/D001773/1, and NE/E01531X/1 and EPSRC Consortium project FRMRC2.

References

Alves M, Gaillard F, Sparrow M, Knoll M, Giraud S (2002) Circulation patterns and transport of the Azores front-current system. Deep-Sea Research II 49:3983-4002

Armi L, Farmer DM (1988) The flow of Mediterranean water through the Strait of Gibraltar. Progress in Oceanography 21:1-105

Bryden HL, Brady EC, Pillsbury RD (1988) Flow through the strait of Gibraltar. In: Almazan JL, Bryden HL, Kinder T, Parilla G (eds) Seminario sobre la Oceanografia fisica del Estrecho de Gibraltar. SECEG, Madrid, pp 166-194

Bryden HL, Kinder T (1991) Steady two-layer exchange through the Strait of Gibraltar. Deep-Sea Research 38:S445-463

Garcia-Lafuente J, Delgado J, Sanchez Roman A, Soto J, Carracedo L, Diaz del Rio G (2009) Interannual variability of the Mediterranean outflow observed in Espartel sill, western Strait of Gibraltar. J Geophys Res 114. doi:10.1029/2009jc005496

Gomis D, Tsimplis MN, Martın-Mıguez B, Ratsimandresy AW, Garcıa-Lafuente J, Josey SA (2006) Mediterranean Sea level and barotropic flow through the Strait of Gibraltar for the period 1958-2001 and reconstructed since 1659. Journal of Geophysical Research-Oceans 111:10.1029/2005JC003186

Gould WJ (1985) Physical Oceanography of the Azores Front. In: Crease J, Gould WJ, Saunders PM (eds) Essays in Oceanography: A tribute to John Swallow. Progress in oceanography. Pergamon Press, Oxford, pp 167-190

Grootes PM, Sarnthein M, Kennett JP, Holbourn A, Nadeau MJ, Kuhn H (2008) Changes in MOC revealed by chronostratigraphic correlation of ocean sediment cores via C-14 plateau tuning. Geochimica Et Cosmochimica Acta 72:A331-A331

Hall IR, Moran SB, Zahn R, Knutz PC, Shen CC, Edwards RL (2006) Accelerated drawdown of meridional overturning in the late-glacial Atlantic triggered by transient pre-H event freshwater perturbation. Geophys Res Lett 33. doi:L16616Artn l16616

Hayes A, Kucera M, Kallel N, Sbaffi L, Rohling EJ (2005) Glacial Mediterranean sea surface temperatures based on planktonic foraminiferal assemblages. Quaternary Science Reviews 24:999-1016

Julien PY (1998) Erosion and Sedimentation. Cambridge University Press, Cambridge

Karim MF, Kennedy JF (1990) Menu of coupled velocity and sediment-discharge relations for rivers. Journal of Hydraulic Engineering 116:978-996

Kuhlemann J, Rohling EJ, Krumrei I, Kubik P, Ivy-Ochs S, Kucera M (2008) Regional synthesis of Mediterranean atmospheric circulation during the last glacial maximum. Science 321:1338-1340. doi:10.1126/science.1157638

Levine RC, Bigg GR (2008) Sensitivity of the glacial ocean to Heinrich events from different iceberg sources, as modeled by a coupled atmosphere-iceberg-ocean model. Paleoceanography 23:16. doi:Pa421310.1029/2008pa001613

Levitus S, Isayev G (1992) Polynomial approximation to the International equation of state for seawater. Journal of Atmospheric and Oceanic Technology 9:705-708

Lynch-Stieglitz J, Adkins JF, Curry WB, Dokken T, Hall IR, Herguera JC, Hirschi JJM, Ivanova EV, Kissel C, Marchal O, Marchitto TM, McCave IN, McManus JF, Mulitza S, Ninnemann U, Peeters F, Yu EF, Zahn R (2007)

Atlantic meridional overturning circulation during the Last Glacial Maximum. Science 316:66-69
McCave IN, Hall IR (2006) Size sorting in marine muds: Processes, pitfalls, and prospects for paleoflow-speed proxies. Geochemistry Geophysics Geosystems 7:Q10N05, doi:10.1029/2006GC001284
McManus JF, Francois R, Gherardi JM, Keigwin LD, Brown-Leger S (2004) Collapse and rapid resumption of Atlantic meridional circulation linked to deglacial climate changes. Nature 428:834-837
MEDATLAS/2002 database. Mediterranean and Black Sea database of temperature salinity and bio-chemical parameters. Climatological Atlas: IFREMER Edition (2002) MEDAR Group
Mikolajewicz U (2010) Modelling Mediterranean ocean climate of the Last Glacial Maximum. Climate of the Past 7:161-180
Millot C (2009) Another description of the Mediterranean Sea outflow. Progress in Oceanography 82:101-124
New AL, Jia Y, Coulibaly M, Dengg J (2001) On the role of the Azores Current in the ventilation of the North Atlantic Ocean. Progress in Oceanography 48:163-194
O'Neill-Baringer M, Price JF (1997) Mixing and spreading of the Mediterranean outflow. Journal of Physical Oceanography 27:1654-1677
O'Neill-Baringer M, Price JF (1999) A review of the physical oceanography of the Mediterranean outflow. Marine Geology 155:63-82
Pinto L, Fortunato AB, Freire P (2006) Sensitivity analysis of non-cohesive sediment transport formulae. Continental Shelf Research 26:1826-1839
Price JF, O'Neill-Baringer M (1994) Outflows and deep water production by marginal seas. Progress in Oceanography 33:161-200
Price JF, O'Neill-Baringer M, Lueck RG, Johnson GC, Ambar I, Parilla G, Cantos A, Kenelly MA, Sanford TB (1993) Mediterranean Outflow Mixing and Dynamics. Science 259:1277-1282
Robinson LF, Adkins JF, Keigwin LD, Southon J, Fernandez DP, Wang SL, Scheirer DS (2005) Radiocarbon variability in the western North Atlantic during the last deglaciation. Science 310:1469-1473. doi:10.1126/science.1114832
Rogerson M, Colmenero-Hidalgo E, Levine RC, Rohling EJ, Voelker AHL, Bigg GR, Schönfeld J, Cacho I, Sierro FJ, Löwemark L, Reguera MI, deAbreu L, Garrick K (2010) Enhanced Mediterranean-Atlantic Exchange During Atlantic Freshening Phases. . Geochemistry Geophysics Geosystems 11:Q08013, doi:08010.01029/02009GC002931
Rogerson M, Rohling EJ, Weaver PPE (2006) Promotion of meridional overturning by Mediterranean-derived salt during the last deglaciation. Paleoceanography 21:10.1029/2006PA001306
Rogerson M, Rohling EJ, Weaver PPE, Murray JW (2005) Glacial to Interglacial Changes in the Settling Depth of the Mediterranean Outflow Plume. Paleoceanography 20:PA3007, doi3010.1029/2004PA001106.
Rogerson M, Schönfeld J, Leng M (2011) Qualitative and quantitative approaches in palaeohydrography: A case study from core-top parameters in the Gulf of Cadiz. Marine Geology 280:150-167
Schönfeld J, Zahn R (2000) Late Glacial to Holocene history of the Mediterranean Outflow. Evidence from benthic foraminiferal assemblages and stable isotopes at the Portuguese margin. Palaeogeography Palaeoclimatology Palaeoecology 159:85-111

Siddall M, Rohling EJ, Almogi-Labin A, Hemleben C, Meischner D, Schmelzer I, Smeed DA (2003) Sea-level fluctuations during the last glacial cycle. Nature 423:853-858

Skinner LC, Elderfield H (2007) Rapid fluctuations in the deep North Atlantic heat budget during the last glacial period. Paleoceanography 22:PA1205, doi:1210.1029/2006PA001338

Stanford JD, Rohling EJ, Hunter SE, Roberts AP, Rasmussen SO, Bard E, McManus J, Fairbanks RG (2006) Timing of meltwater pulse 1a and climate responses to meltwater injections. Paleoceanography 21:PA4103, doi:4110.1029/2006PA001340

Voelker AHL, Lebreiro SM, Schoenfeld J, Cacho I, Erlenkeuser H, Abrantes F (2006) Mediterranean outflow strengthening during northern hemisphere coolings: A salt source for the glacial Atlantic? Earth and Planetary Science Letters 245:39-55

Table 1. Monte Carlo variables used in modified PO94 model for Figures 1 and 2.

Parameter	Modern value	Monte Carlo parameterisation
Sea Level	0m	Monotonic random value between 0 and -130.
X_{Med}	0.05	Monotonic random value between 0.025 and 0.1
Winter Sea Surface Temperature (wSST) in Atlantic inflow.	16^{o}C	Monotonic random value between 7 and 20^{o}C.
Temperature difference between MIW and wSST.	~4^{o}C	Monotonic random value between 0 and 6^{o}C.
Temperature difference between MDW and wSST.	~4.5^{o}C	Monotonic random value between 0 and 6^{o}C (must exceed difference for MIW so that MDW is the coldest Mediterranean watermass)
Proportional admixture of MDW in MO	~0.3	Monotonic random value between 0 and 1.
Density gradient in mid-latitude eastern North Atlantic	0.0009 kg m^{-4}	Monotonic random value between 0.00009 and 0.0018.

Table 2. Boundary conditions for scenario simulations (Figure 4).

Parameter	Upper limit	Lower limit
Holocene		
AMW settling depth (m)	500	1100
Sea Level (m)	0	-10
Surface Temperature (^oC)	18	16
Western Med. Cooling (^oC)	3	0
Eastern Med. Cooling (^oC)	3	0
X_{Med} (Sv)	0.05	0.04
Bølling-Allerød		
AMW settling depth (m) (Schönfeld and Zahn 2000)	800	1000
Sea Level (m)	-70	-90
Surface Temperature (^oC)	16	12
Western Med. Cooling (^oC)	3	0
Eastern Med. Cooling (^oC)	3	0
X_{Med} (Sv)	0.05	0.04
Younger Dryas		
AMW settling depth (m) (Schönfeld and Zahn 2000)	1300	1500
Sea Level (m)	-50	-70
Surface Temperature (^oC)	14	10
Western Med. Cooling (^oC)	6	0
Eastern Med. Cooling (^oC)	6	0
X_{Med} (Sv)	0.05	0.04
LGM		
AMW settling depth (m) (Schönfeld and Zahn 2000)	1400	2000
Sea Level (m)	-100	-130
Surface Temperature (^oC)	14	10
Western Med. Cooling (^oC)	6	0
Eastern Med. Cooling (^oC)	6	0
X_{Med} (Sv)	0.05	0.04
Heinrich Event 1		
AMW settling depth(m) (Skinner and Elderfield 2007)	2000	2600
Sea Level (m)	-100	-130
Surface Temperature (^oC)	9	6
Western Med. Cooling (^oC)	6	0

Eastern Med. Cooling (^{o}C)	6	0
X_{Med} (Sv)	0.1	0.025

Table 3. List of parameters used in this study.

Symbol	Parameter	Value (if constant)	Units
Φ	Mixing coefficient		
B_{geo}	Geostrophic Buoyancy Flux		$m^3\ s^{-3}$
U_{geo}	Geostrophic Velocity		$m\ s^{-1}$
g'	Reduced gravity		
π	Bottom gradient		^{o}
f	Coriolis parameter	0.000084	
H_{src}	Height of MOW plume at source		m
K_{geo}	Geostrophic Ekman number		
x	Distance from source of entrainment "event"	100,000	m
W_{src}	Width of MOW plume at source		m
g	Acceleration due to gravity	9.81	$m\ s^{-2}$
ρ_{MO}	Density of Mediterranean Water		$kg\ m^{-3}$
ρ_{ATL}	Density of inflowing Atlantic Water		$kg\ m^{-3}$
$D_{settling}$	Mean settling depth of AMW		m
$\Delta\rho_{MO}$	Density difference of Mediterranean and Atlantic water		$kg\ m^{-3}$
D_s	Depth of water at the Camarinal Sill.		m
H'	Global Sea Level change		m
$\partial\rho / \partial z$	Atlantic vertical density gradient		$kg\ m^{-4}$
Q_{MO}	Flux of MOW		Sv
ΔS_{gib}	Salinity difference between Atlantic and Mediterranean Water		PSU
S_{atl}	Salinity of inflowing Atlantic water		PSU
X_{med}	Mediterranean net freshwater export flux		Sv
C	Geometric coefficient for Strait of Gibraltar	0.283	
Q_{total}	Total, two-layer export at Gibraltar		Sv
β	Coefficient of saline contraction	0.00077	$kg\ m^{-3}\ PSU^{-1}$
α	Coefficient of thermal expansion	0.0002	$kg\ m^{-3}\ {}^oC^{-1}$
ΔT_{gib}	Temperature difference between Atlantic and Mediterranean Water		^oC
q_s	Sediment flux		$kg\ s^{-1}$
x1	First entrainment coefficient		
x2	Second entrainment coefficient		
s_d	Sediment density	2.65	$g\ cm^{-3}$
d_{50}	median grainsize of sediment	2.4	μm
U*	Shear velocity		$m\ s^{-1}$
U^*_{crit}	Critical Shear Velocity	2.4	$m\ s^{-1}$

Figure Captions

Figure 1: a; Vertical density structure of the North Atlantic in the region between 12 and 8^{o}W and 33 and 38^{o}N. Observations of past AMW activity (Schönfeld and Zahn 2000; Skinner and Elderfield 2007) are also shown. b-f show the estimated impact on settling depth of the AMW plume from the Monte Carlo-like model derived from: b, net freshwater flux from the Mediterranean (X_{Med}); c, cooling effects in the Gulf of Lions; d, cooling effects in the eastern Mediterranean; e, sea level change. 1f, shows the range of shear velocities (U*) for the range of settling depths produced by the model. Shear velocities exceeding 2.4 m s^{-1} (shown by the vertical line) are capable of entraining sediment and those exceeding 6.8 m s^{-1} imply hyperconcentration of sediment. For these simulations, sediment concentration is capped at 5% by volume.

Figure 2 a-c; Modelled increase in AMW settling depth due to sediment entrainment (see Fig. 1f): a, relation to sea level change; b, relation to bottom water temperatures; c, relation to reduced density of the AMW plume (g'). Fig. 2d-f, output of the Monte Carlo-like model when the Atlantic vertical density is allowed to vary randomly between 0.5 and 2 times the modern value: d, control of settling depth by net freshwater flux from the Mediterranean (X_{Med}); e, control from sea level change; f, control from Atlantic vertical density gradient ($\partial\rho$ / ∂z).

Figure 3; Hydrographic and GCM (Levine and Bigg 2008) output showing vertical density gradient in the eastern North Atlantic in a 10^{o} box with its northeast corner at Cape St Vincent. Grey points are hydrographic data (MEDATLAS 2002). Red circles are GCM output for present day, blue circles are GCM output for LGM and black stars are GCM output during a Hudson Strait Heinrich iceberg flux experiment. GCM data have been adjusted so that density at 300m is compatible with hydrographic data.

Figure 4; a: Probabilistic assessment of Atlantic vertical density gradient during the late Holocene (unfilled, broken lines), Bölling-Allerod (grey fill), Younger Dryas (red fill), LGM (black fill), LGM with sediment entrainment impact (unfilled, green line) and Heinrich Event 1 (blue fill). Boundary conditions for simulations presented in Supporting Table 2. Fig 4b: Black data is simulation hydrographic data for LGM scenario, grey data show simulations incorporating the impact of sediment entrainment.

Figure 1

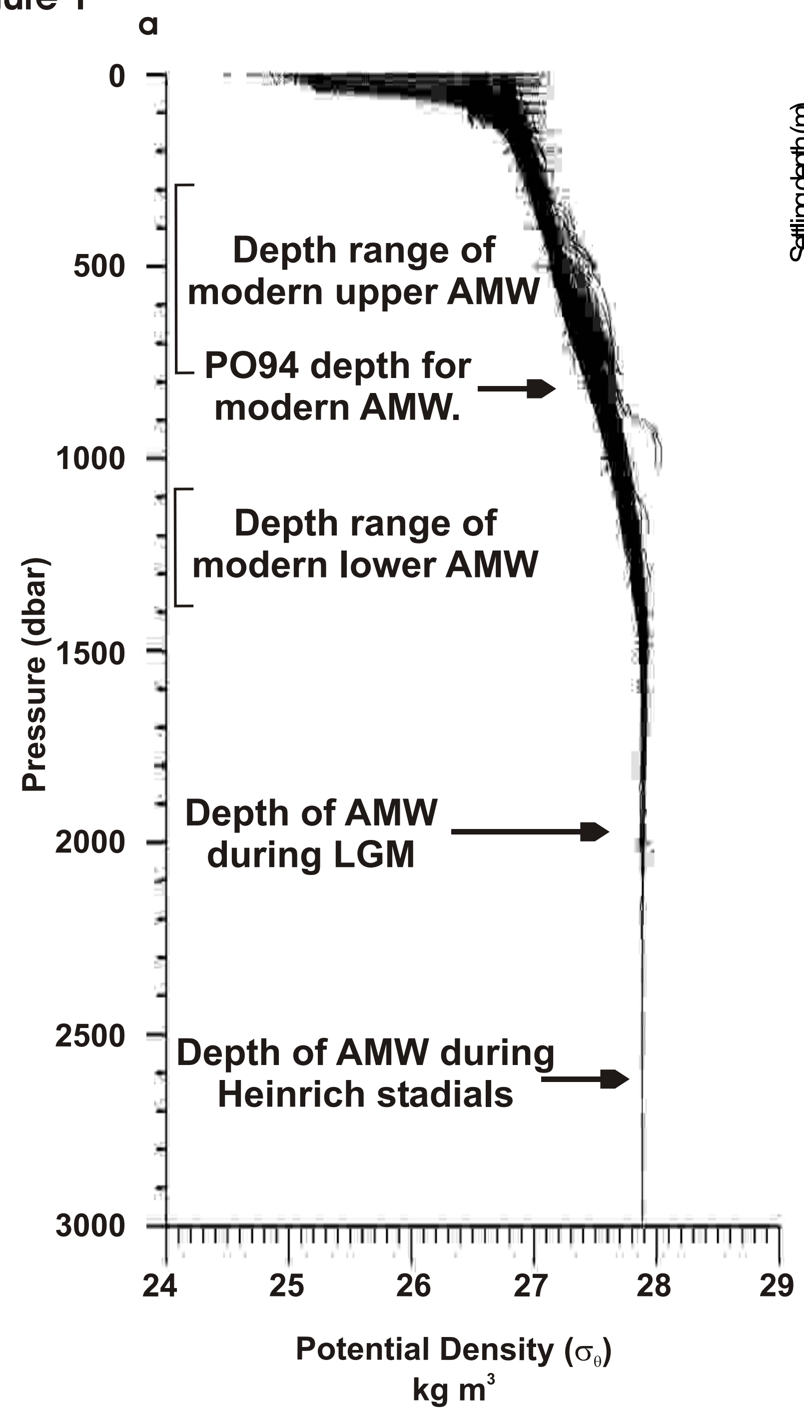
a
Pressure (dbar)
0
500
1000
1500
2000
2500
3000
Depth range of modern upper AMW
PO94 depth for modern AMW.
Depth range of modern lower AMW
Depth of AMW during LGM
Depth of AMW during Heinrich stadials
24
25
26
27
28
29
Potential Density (σθ) kg m3
b
R2 = 0.85
Settling depth (m)
Xmed (Sv)
c
Difference between SST and TMDW (oC)
d
Difference between SST and TMIW(oC)
e
Sea level change (m)
f
U* (m s-1)

Figure 2

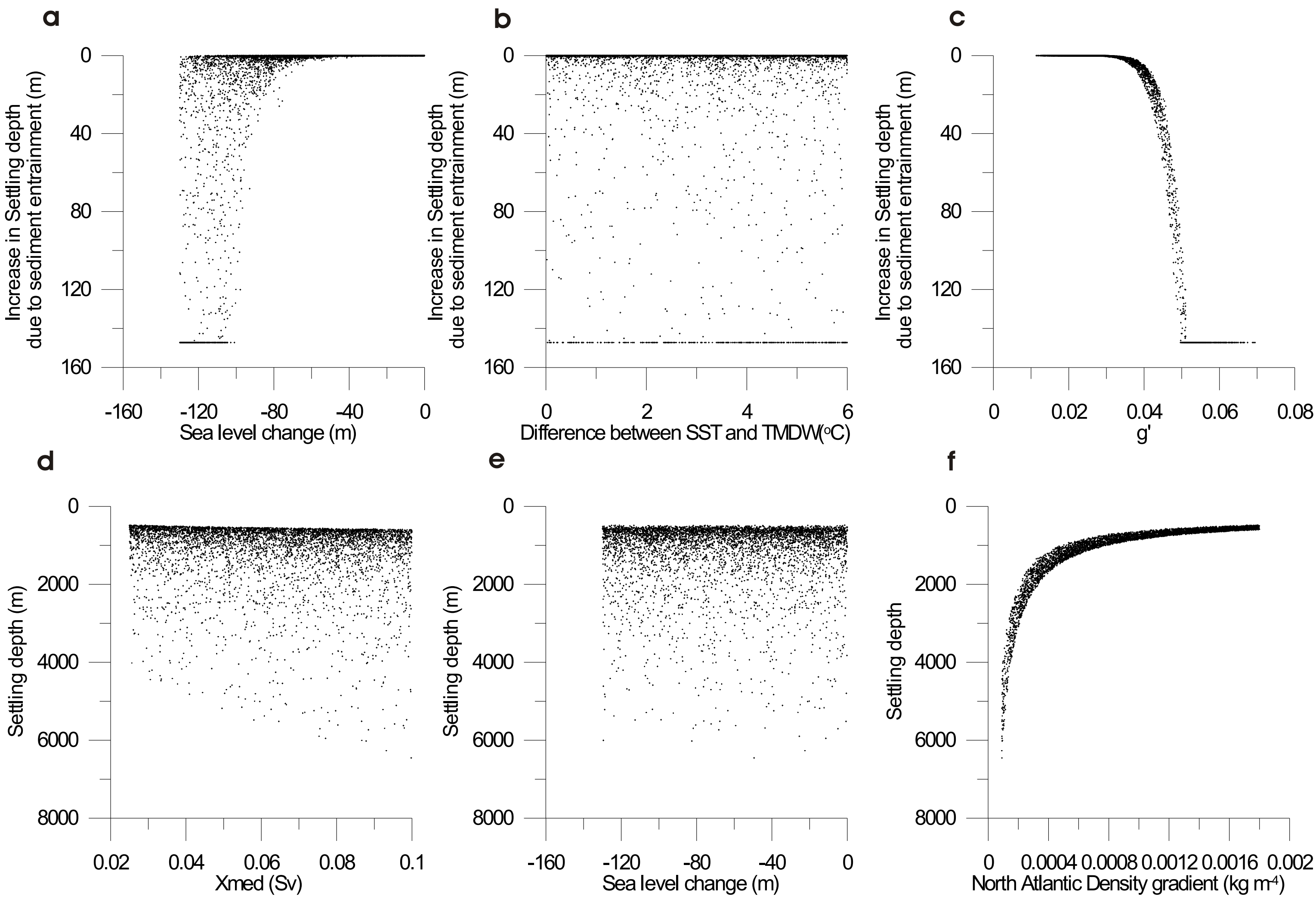

a
b
c
Increase in Settling depth due to sediment entrainment (m)
0
40
80
120
160
-160
-120
-80
-40
0
Sea level change (m)
0
2
4
6
Difference between SST and TMDW(°C)
0
0.02
0.04
0.06
0.08
g'
d
e
f
Settling depth (m)
0
2000
4000
6000
8000
0.02
0.04
0.06
0.08
0.1
Xmed (Sv)
Sea level change (m)
Settling depth
0
0.0004
0.0008
0.0012
0.0016
0.002
North Atlantic Density gradient (kg m-4)

Figure 3

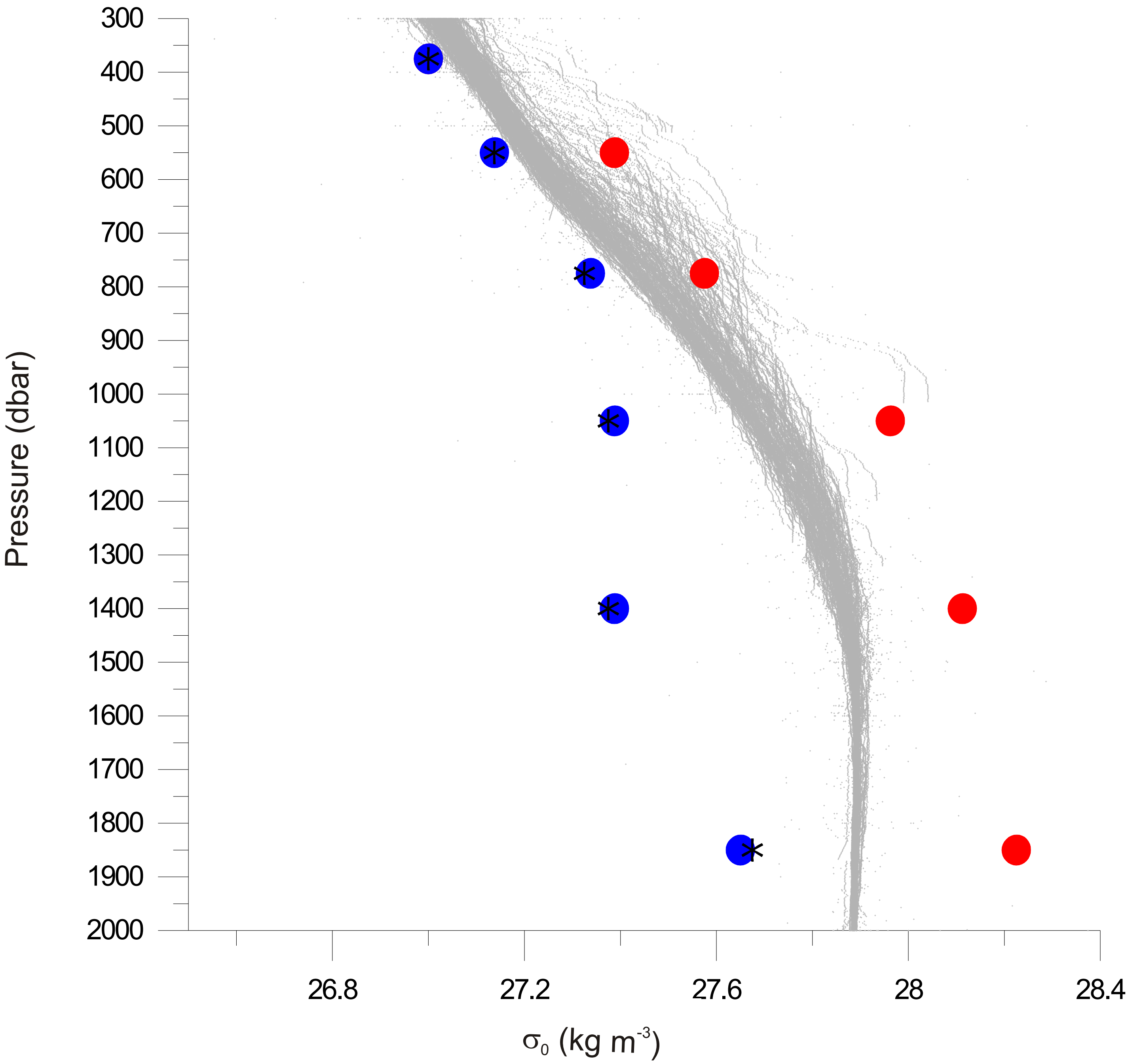

Pressure (dbar)
300
400
500
600
700
800
900
1000
1100
1200
1300
1400
1500
1600
1700
1800
1900
2000
26.8
27.2
27.6
28
28.4
σ_0 (kg m^{-3})

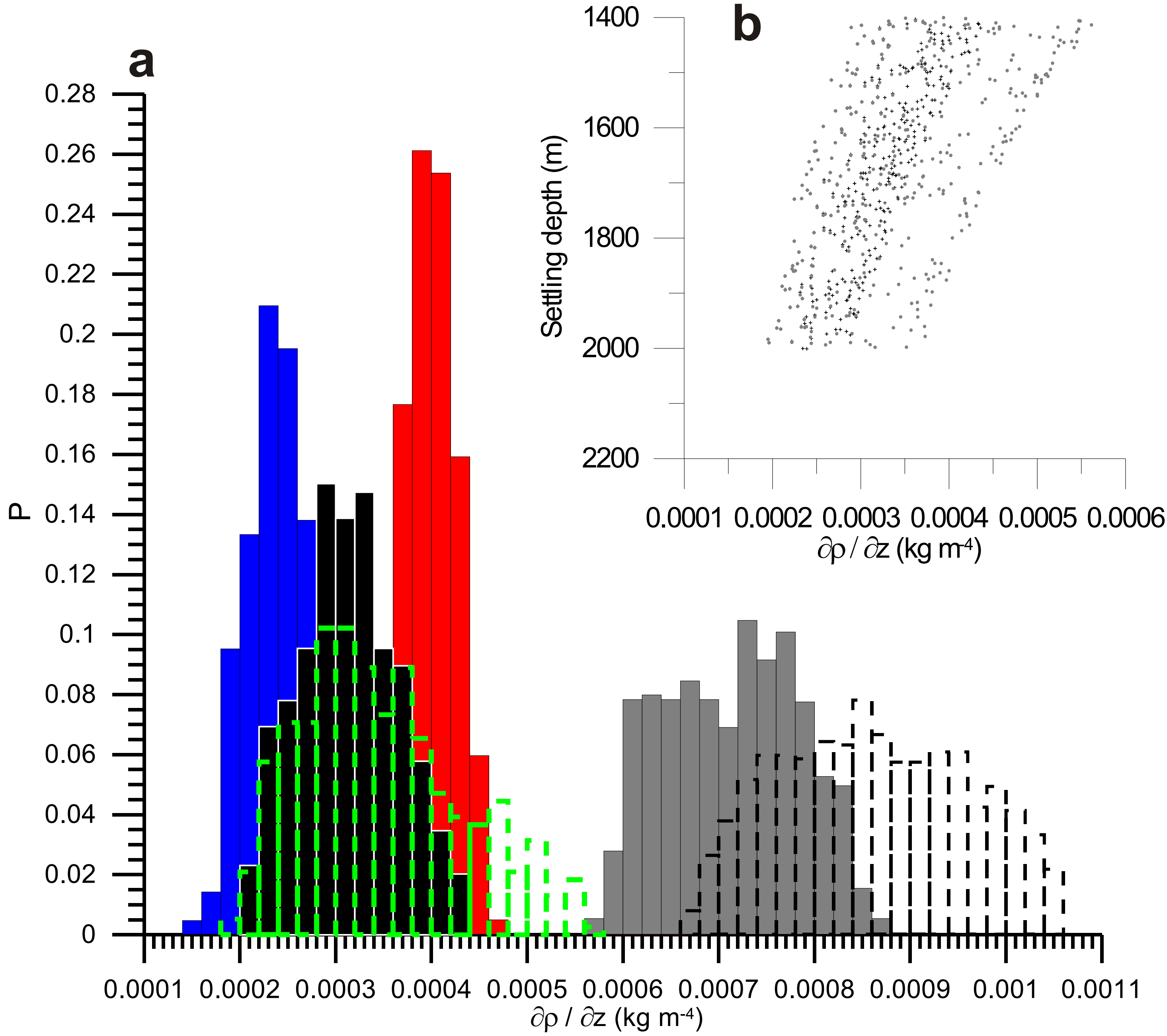

a
P
0.28
0.26
0.24
0.22
0.2
0.18
0.16
0.14
0.12
0.1
0.08
0.06
0.04
0.02
0
0.0001 0.0002 0.0003 0.0004 0.0005 0.0006 0.0007 0.0008 0.0009 0.001 0.0011
∂ρ / ∂z (kg m-4)
b
Settling depth (m)
1400
1600
1800
2000
2200
0.0001 0.0002 0.0003 0.0004 0.0005 0.0006
∂ρ / ∂z (kg m-4)